arXiv:0812.4294v2 [cond-mat.mtrl-sci] 21 May 2009

Re-examination of half-metallic ferromagnetism for doped $LaMnO_3$ in quasiparticle self-consistent GW method

Takao Kotani
*Faculty of engineering, Tottori university, Tottori 680-8552, Japan**

Hiori Kino
National Institute for materials science, Sengen 1-2-1, Tsukuba, Ibaraki 305-0047, Japan.

(Dated: May 21, 2009)

We apply the quasiparicle self-consistent GW (QSGW) method to a cubic virtual-crystal alloy $La_{1-x}Ba_xMnO_3$ as a theoretical representative for colossal magnetoresistive perovskite manganites. The QSGW predicts it as a fully-polarized half-metallic ferromagnet for a wide range of x and lattice constant. Calculated density of states and dielectric functions are consistent with experiments. In contrast, the energies of calculated spin wave are very low in comparison with experiments. This is affected neither by rhombohedral deformation nor the intrinsic deficiency in the QSGW method. Thus we ends up with a conjecture that phonons related to the Jahn-Teller distortion should hybridize with spin waves more strongly than people thought until now.

PACS numbers: 75.47.Gk 71.15.Qe 71.45.Gm

I. INTRODUCTION

The mixed-valent ferromagnetic perovskite $La_{1-x}A_xMnO_3$, where A is an alkaline-earth such as Ca, Sr or Ba, shows the colossal magnetresistence, e.g, see reviews by Tokura and Nagaosa [1], and by Imada, Fujimori and Tokura [2]. As they explain, the colossal magnetresitance is related to the complexed interplay of spin, orbital and lattice degree of freedoms. This is interesting not only from a view of physics, but also of its potential applicabilities. This interplay can be also related to the fundamentals of high-T_c superconductors and the multiferroic materials, which are now intensively being investigated [3, 4].

In order to understand the interplay, kinds of theoretical works have been performed until now. They can be classified into two approaches; one is model approaches, and the other is the first-principle ones which are mainly based on the density functional theory in the local density approximation (LDA) or in the generalized gradient approximation (GGA) [5, 6, 7, 8, 9]. The first-principle approaches have an advantage that it can give energy bands (as quasiparticles) without any knowledge of experimental input. Then kinds of properties are calculated based on the quasiparticles. However, it is well known that the density functional theory in the LDA (and GGA) often fails to predict physical properties for compounds including transition metals. For example, Terakura, Oguchi, Williams and J. Kübler [10, 11] showed that the density functional theory in the LDA is only qualitatively correct for MnO and NiO. Calculated band gaps and exchange splittings are too small, resulting in poor agreement with optical and spin wave experiments [12, 13, 14, 15]. This is little improved even in the GGA.

As a remedy, the LDA+U method has been often used [16]. However, it has the same shortcomings as model calculations: It can contain many parameters which are not determined within the theory itself, e.g, different U for t_{2g} and e_g orbitals [6, 17] and U for O($2p$) (oxygen $2p$)[18]. Even though there are theoretical efforts in progress to evaluate these U parameters in first-principle methods [19, 20], we now usually have to determine these parameters by hand so as to reproduce some experiments in practice. Then we need to check whether calculations with the parameters can explain other experiments or not.

Many researches are performed along this line. Soloveyv et al. investigated $LaTO_3$(T=Ti-Cu) in the LDA+U, where they tested possible ways of LDA+U in comparison with experiments. Then they concluded that LDA+U gives little differences from the results in the LDA in the case of $LaMnO_3$. It followed by their successful description of the spin-wave dispersions [7] and phase diagrams [8] in the LDA even for $x \neq 0$. Ravindran et al. also showed detailed examination for $LaMnO_3$ with full-potential calculations including spin-orbit coupling and full distortion of crystal structure [9], where they concluded that the density functional theory in the GGA worked well for $LaMnO_3$. Thus, both of these groups reached to the same conclusion that "We can treat $La_{1-x}A_xMnO_3$ accurately enough with the density functional theory in the LDA or in the GGA, do not need to use LDA+U.". It sounds very fortunate because we are not bothered with difficulties about how to determine parameters U in the LDA+U. However, we must check this conclusion carefully. For example, one of the reason why the GGA is accurate is based on their observation that their calculated imaginary part of dielectric function $\epsilon_2(\omega)$ in the GGA agrees well with an experiment [9]. However, this is not simply acceptable if we recall other cases where peaks in the calculated $\epsilon_2(\omega)$ are deformed and pulled down to lower energies when we take into ac-

*moved from Arizona State University, Tempe, USA

count excitonic effects. Thus it is worth to re-examine the conclusion by some other methods which are better than those dependent on the LDA or the GGA.

Here we re-examine the conclusion by the quasiparticle self-consistent GW (QSGW) method, which is originally developed by Faleev, van Schilfgaarde, and Kotani [12, 13]. Its theoretical and methodological aspects, and how it works are detailed in [13] and references there in. They showed that the QSGW method gave reasonable results for wide-range of materials.

In Sec.II, we explain our method. Then we give results and discussions in Sec.III. In our analysis in comparison with experiments, calculated quasiparticle energies given by the QSGW seems to be consistent with experiments. However, the obtained spin wave energies are about four times too larger than experimental values. From these fact, as for $La_{1-x}A_xMnO_3$, we ends up with a conjecture that phonons related to the Jahn-Teller distortion should hybridize with spin waves more strongly than people thought until now. This is our main conclusion presented at the end of Sec.III.

II. METHOD

We first explain the QSGW method which is applied to calculations presented in this paper.

The GW approximation (GWA) is a perturbation method. Generally speaking, we can perform GWA from any one-body Hamiltonian H^0 including non-local static potential $V^{\rm eff}(\mathbf{r},\mathbf{r}')$ as

$$H^0 = \frac{-\nabla^2}{2m} + V^{\rm eff}(\mathbf{r},\mathbf{r}'). \quad (1)$$

The GWA gives the self-energy $\Sigma(\mathbf{r},\mathbf{r}',\omega)$ as a functional of H^0; the Hartree potential through the electron density is also given as a functional of H^0. Thus GWA defines a mapping from H^0 to $H(\omega)$, which is given as $H(\omega) = \frac{-\nabla^2}{2m} + V^{\rm ext} + V^{\rm H} + \Sigma(\mathbf{r},\mathbf{r}',\omega)$. Here $V^{\rm ext}$ and $V^{\rm H}$ denote the external potential from nucleus and the Hartree potential symbolically. In other words, the GWA gives a mapping from the non-interacting Green's function $G_0 = 1/(\omega - H^0)$ to the interacting Green' function $G = 1/(\omega - H(\omega))$.

If we have a prescription to determine H^0 from $H(\omega)$, we can close a self-consistency cycle; that is, $H^0 \to H(\omega) \to H^0 \to H(\omega) \to ...$ (or $G_0 \to G \to G_0 \to ...$, equivalently) can be repeated until converged. One of the simplest example of the prescription is to use $H(\omega)$ at the Fermi energy $E_{\rm F}$, that is, $H^0 = H(E_{\rm F})$ for $H(\omega) \to H^0$. In practice, we take a better choice in the QSGW method so as to remove the energy-dependence; we replace $\Sigma(\mathbf{r},\mathbf{r}',\omega)$ with the static version of self-energy $V^{\rm xc}(\mathbf{r},\mathbf{r}')$, which is written as

$$V^{\rm xc} = \frac{1}{2}\sum_{ij} |\Psi_i\rangle \left\{ {\rm Re}[\Sigma(\varepsilon_i)]_{ij} + {\rm Re}[\Sigma(\varepsilon_j)]_{ij} \right\} \langle\Psi_j|, \quad (2)$$

where $\{\varepsilon_i\}$ and $\{\Psi_i\}$ are eigenvalues and eigenfunction of H, and $\Sigma(\varepsilon_i) = \langle\Psi_i|\Sigma(\varepsilon_i)|\Psi_j\rangle$. Re$[X]$ means taking only the Hermitian part of the matrix X. With this $V^{\rm xc}$, we can generate a new H^0, that is, it gives a procedure $H^0 \to H \to H^0$. Thus we now have a self-consistency cycle. By construction, the eigenvalues of H^0 is in agreement with the pole positions of $H(\omega)$. Thus the eigenvalue is directly interpreted as the quasiparticle energies. This QSGW method is implemented as an extension of an all-electron full-potential version of the GW method [21] as detailed in [13].

Until now they have shown that QSGW works well for kinds of materials (see [13, 22] and references there in). In [21], Kotani and van Schilfgaarde have shown that the ordinary one-shot GW based on the LDA systematically gave too small band gaps even for semiconductors; this is confirmed by other theorists [23, 24]. Thus the self-consistency is essentially required to correct such too small band gaps[13, 25]. Furthermore, the adequacy of one-shot GW is analyzed from kinds of view points in [26]; e.g., it shows that the usual one-shot GW can not open the band gap for Ge as shown in its Fig.6 (band entanglement problem). The self-consistency is especially important for such as transition metal oxides like $La_{1-x}A_xMnO_3$ when reliability of the LDA and the GGA is questionable. We have shown that QSGW works well for wide range of materials including MnO and NiO [12, 13, 22, 25, 27, 28]. We observed still remaining discrepancies between the QSGW and experimental band gaps, but they are systematic and may be mainly corrected by including the electron-hole correlation in the screened coulomb interaction W as shown by Shishkin, Marsman and Kresse [23].

In this paper, we focus on these two objectives:

(i) Difference of results in the QSGW and in the LDA.

(ii) Are results in the QSGW consistent with experiments? If not, what can the results mean?

For these objectives, we mainly treat the simplest cubic structure of the perovskite, one formula unit per cell, for $La_{1-x}A_xMnO_3$, where we set A as Ba in a virtual atom approximation, that is, $La_{1-x}Ba_x$ is treated as a virtual atom with the atomic number $Z = 57 - x$. We use $6\times6\times6$ $\mathbf{k}$ points in the 1st Brillouin zone (BZ) for integration. We also treat a rhombohedral case for $x = .3$ (two formula units per cell. Its structure is taken from [29]; angle of Mn-O-Mn is ~ 170 degree) to examine the effect due to the rotation of oxygen-octahedra (this is not a Jahn-Teller distortion). Neither phonon contributions nor the spin-orbit coupling are included in all presented calculations.

Because of the difficulty to apply the GW method to systems with localized d electrons, even the one-shot GW calculations were rarely applied to $La_{1-x}A_xMnO_3$ until now. Within our knowledge, one is by Kino et al [30], and the other is by Nohara et al [31]. Both are only within the atomic sphere approximation for one-body potential. In

contrast, our method is in a full-potential method. Thus our method here is superior to these works in this point, and in the self-consistency in the QSGW.

III. RESULTS AND DISCUSSIONS

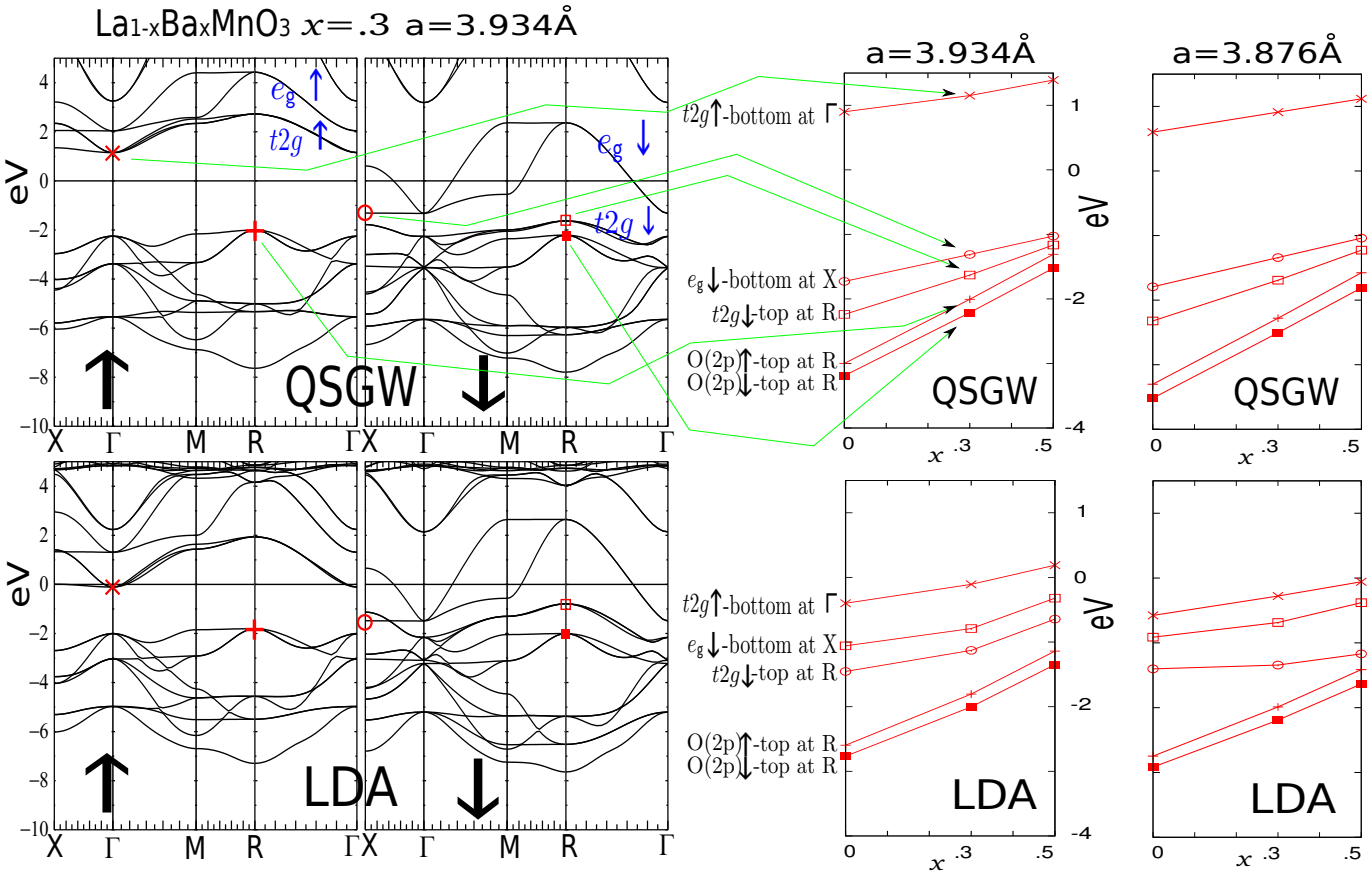

FIG. 1: (color online) The left panels are energy band at $x = 0.3$ in QSGW and in LDA for the lattice constant, a=3.934Å(as used in [7]) in the black solid lines. The Fermi energy $E_{\rm F}$ is at 0 eV. Right four panels show five typical eigenvalues for different x, not only for a=3.934Å, but also for a=3.876Å. Those are shown by (red) symbols ×, +, ◯, □, and ■. Correspondence to those in the left panels are indicated by thin (green) lines with arrows.

In the left half of Fig.1, we compare energy bands in the QSGW and in the LDA at $x = 0.3$ for lattice constant a=3.934Å. The energy bands are roughly assigned as O($2p$), t_{2g}, and e_g bands from the bottom. In its upper panels, we show labels t_{2g} and e_g to show the assignments. The QSGW gives a band gap in the minority spin (↑), that is, it is a half-metal, though the LDA does not. This enhancement of half-metallic feature in GWA is already reported even in the one-shot GW calculations by Kino et al [30]. Its implication is emphasized in a recent review for half-metallic ferromagnet by Katsnelson et al [32]. The width of the $e_g\downarrow$ band in the QSGW shows little difference from that in the LDA. In the QSGW, the $t_{2g}\downarrow$ band, which is hybridized with O($2p$)↓, becomes narrower and deeper than that in the LDA.

Right half of Fig.1 shows five typical eigenvalues as function of x, not only for a=3.934Å, but also for a=3.876Å. In all cases treated here, $t_{2g}\uparrow$-bottom at Γ (bottom of conduction band for ↑) is above $E_{\rm F}$ ($E_{\rm F}$ is at 0 eV), and O(2p)↑-top at R (top of valence band for ↑) is below $E_{\rm F}$ in QSGW. This means that it becomes fully-polarized half metals in the QSGW (thus the magnetic moment is given as $4 - x$ $\mu_{\rm B}$). In contrast, the LDA gives a fully polarized half metal only when $x = 0.5$ for $a = 3.934$Å ($t_{2g}\uparrow$-bottom is slightly above $E_{\rm F}$). The eigenvalues of $t_{2g}\downarrow$-top at R are very close to that of O($2p$)↓-top at R in the QSGW, especially for large x. Though the QSGW eigenvalues show linear dependencies as a function of x, the LDA does not. This is because the LDA has a small occupancy for the $t_{2g}\uparrow$ band.

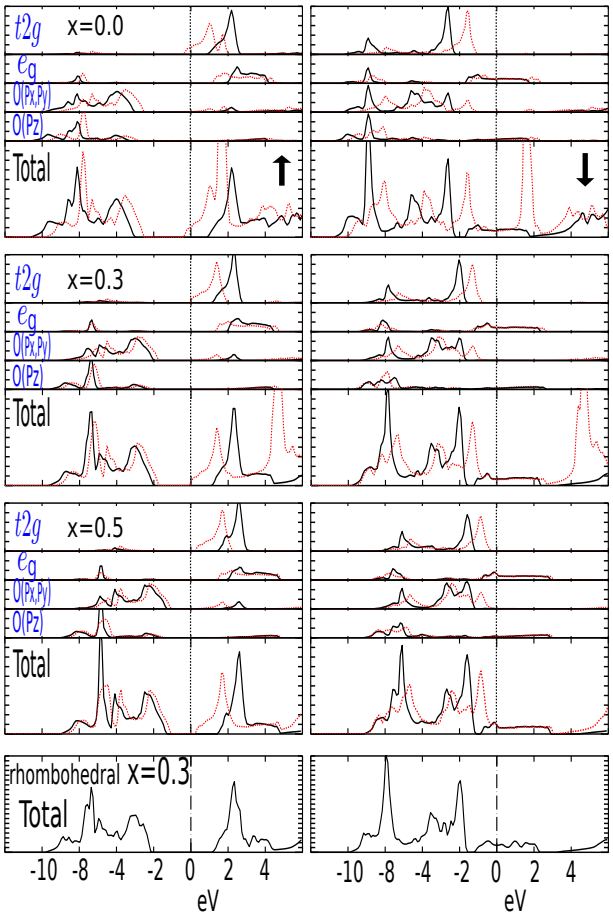

FIG. 2: (color online) Density of states in QSGW (black solid line) and LDA(red dotted line) for a=3.934Å. $E_{\rm F}$ is at 0 eV. Left panels are for minority spin, and right panels are for majority spin. Four panels from the top to the bottom are for $x = 0.0$, $x = 0.3$, $x = 0.5$, and for the rhombohedral cases, respectively. The $4f$ band in QSGW is above the plotted region here in QSGW. O(p_z) denotes O($2p$) orbitals along Mn-O-Mn. O(p_x,p_y) are perpendicular to O(p_z).

Fig. 2 shows the corresponding total and partial density of states (DOS). O(p_z) denote O($2p$) orbitals along Mn-O-Mn bonding (for σ-bonding with $e_{\rm g}$ orbitals). At first, La($4f$) level is located too low in LDA, at only $\sim$1.5eV above $E_{\rm F}$ for $x = 0$ [5], though the QSGW pushes it up to $\sim E_{\rm F}$+10 eV. At $x = 0$, all peak positions in QSGW show some disagreement with those in the LDA. This is due to the large difference in the occupation for the $t_{2g}\uparrow$ band. On the other hand, for $x = 0.3, 0.5$, we see that differences of the total DOS are mainly for a peak at $\sim E_{\rm F}-2$eV in $\downarrow$, and a peak at $\sim E_{\rm F}+2$eV in $\uparrow$. The former difference is related to the the $t_{2g}\downarrow$ level. If we push down the LDA $t_{2g}\downarrow$ level by $\sim$0.8eV, the occupied bands will be closer to those in QSGW. The latter difference is related to both of the unoccupied Mn($3d$) ($t_{2g}\uparrow$ and $e_{\rm g}\uparrow$). The QSGW pushes up $t_{2g}\uparrow$ and $e_{\rm g}\uparrow$ by $\sim$ 1eV, relative to the LDA results. The experimental position of $t_{2g}\downarrow$ band is described well in the QSGW than the LDA as follows. Angle resolved photo emission spectroscopy (ARPES) by Liu et al [33] concluded that Mn($3d$) band (presumably due to $t_{2g}\downarrow$) is $\sim$ 1eV deeper than the LDA result for $La_{.66}Ca_{0.33}MnO_3$. Chikamatsu et al [34] also performed ARPES for $La_{0.6}Sr_{0.4}MnO_3$, showing that there is a flat dispersion around $E_{\rm F}-2$eV. These experiments for $t_{2g}\downarrow$ support the results in the QSGW. As for the positions of the unoccupied Mn($3d$) bands, no inverse photoemisson experiments are available to identify them though we give some discussion below when we show ϵ_2.

As we see above, the main difference between the QSGW and the LDA is interpreted as the difference of the exchange splitting for the t_{2g} band. Roughly speaking, center of $t_{2g}\downarrow$ and $t_{2g}\uparrow$ given in the LDA is kept in the QSGW. Because of the larger exchange splitting, QSGW shows large half-metallic band gaps. In addition, the $e_{\rm g}\uparrow$ band is pushed up. Based on the knowledge in other materials together with the above experiments, we think that the QSGW should give better description than the LDA. Generally speaking, LDA can introduce two types of errors when we identify the Kohn-Sham eigenvalues with the quasiparticle energies. One is the U-type effect as in LDA+U. This is onsite contribution for localized orbitals. The other is the underestimation of the band gap for extended orbitals as in semiconductors (In the case of diatomic molecule, non-locality in the exchange term can distinguish bonding and anti-bonding orbitals, though onsite U can not). As seen in [13], QSGW can correct these two at the same time without any parameters by hand.

Fig.3 shows ϵ_2 in comparison with the experiment [35] for $La_xSr_{1-x}MnO_3$. The LDA seemingly gives reasonable agreement with the experiment. For example, the peak position around 4eV, which is mainly due to transitions within the $\uparrow$ channel, seemingly give excellent agreement with the experiment (upper panel). This is consistent with the conclusion by Ravindran et al [9]. On the other hand, ϵ_2 in the QSGW makes peak positions located at higher energies than the experiment by $\sim$ 1eV. However, this kind of disagreement is what we observed in other materials[13], where we identified two causes making the difference; (a) A little too high unoccupied quasiparticle energies in the QSGW and (b) The excitonic effect which is related to the correlation motion of electrons and holes during the polarization (we need to solve the Bethe-Salpeter equation). As for (a), we have an empirical procedure to estimate the error due to (a); a simple empirical linear mixing procedure of 80% of $V^{\rm xc}$(Eq. (2)) with 20 % of the LDA exchange-correlation practically worked well as shown in [22, 28]. We have applied this to the case for $x = 0.3$ and $a = 3.934$. Then the $t_{2g}\downarrow$ level ($\times$ in Fig. 1) is reduced from 1.15eV to 0.93eV. This level of overestimation 0.2 $\sim$ 0.3eV is ordinary for band gaps of semiconductors [25]. If this estimation is true, the main cause of the disagreement should be due to (b). We think this is likely because we expect large excitonic effects due to localized electrons. At least, the disagreement in Fig.3 do not mean the inconsistency of the QSGW results with

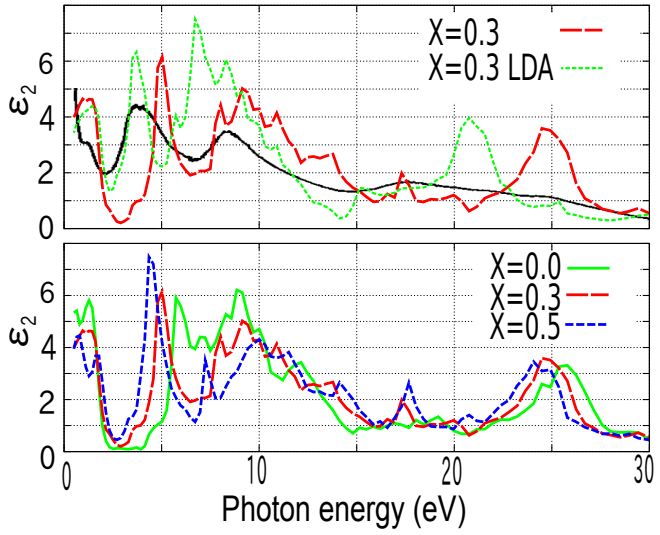

FIG. 3: (color online) Imaginary part of the dielectric function ϵ_2 for a=3.934Å. Local-field correction is neglected but it should be negligible as in the case of MnO and NiO [13]. Upper panel is to compare calculations in QSGW and in LDA with an experiment for $La_{0.3}Sr_{0.7}MnO_3$ [35] by black solid line. In lower panel, we show results in QSGW for different x. Because of a limit in our computational method, ϵ_2 for < 0.5eV are not calculated (In practice, our results are with the wave vector $\mathbf{q} = \frac{2\pi}{a}(0, 0, 0.04)$ instead of $\mathbf{q} = 0$, though we confirmed little changes even at $\mathbf{q} \to 0$.)

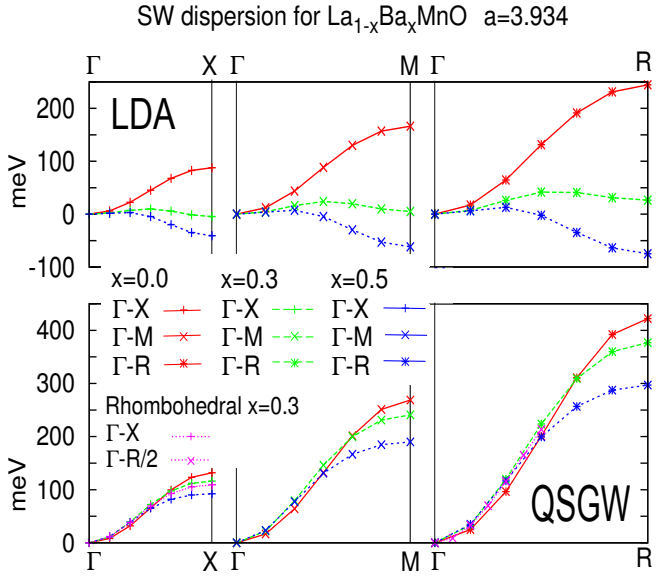

FIG. 4: (color online) Spin wave dispersion along Γ-X, Γ-M, and Γ-R lines for a=3.934Å. Negative energy means the unstable modes. We also superpose the spin-wave dispersion in a rhombohedral case for $x = 0.3$ by pink lines (only Γ-X and Γ-R/2 in the QSGW panels). It is almost on the cubic case, where R/2=(0.25,0.25,0.25) in cubic structure is on the BZ boundary of the rhombohedral structure.

the experiment, though we need further research on it in future. In addition, the effect due to the virtual crystal approximation is unknown. We have also calculated ϵ_2 for rhombohedral structure, resulting in very small differences from that for the cubic one. The lower panel in Fig.3 shows changes as a function of x. Its tendency as function of x (the first peak at ∼5eV is shifted to lower energy, and the magnitude of the second peak at ∼ 9eV is reduced for larger x) is consistent with the experiment [35].

Let us study the magnetic properties. As discussed in [7], the exchange interaction is mainly as the sum of the ferromagnetic contribution from the e_g bands, and the anti-ferromagnetic one from the t_{2g} bands. By the method in [15], where the spin wave calculation based on the QSGW reproduced experimental results very well for MnO and NiO, we obtain the spin wave dispersions as shown in Fig. 4. The method is in a random-phase approximation to satisfy (spin wave energy) $\to$ 0 at the wave vector $\mathbf{q} \to 0$. In the LDA, the ferromagnetic ground state is stable at $x = 0$, but it becomes unstable at $x \gtrsim 0.3$. This is consistent with the result by Soloveyv et al [7], though our LDA results are a little smaller than those for larger x. On the other hand, we found that the ferromagnetic state is stable even at large x in the QSGW: Roughly speaking, the spin wave energies in the QSGW are about four times larger than experimental results [36]. We also show the spin waves for the rhombohedral case in Fig. 4 (along Γ-X and along Γ-R/2), but they are almost on the same line in the cubic case. This means that the rotation of the oxygen tetrahedra gives little effects for its magnetic properties. In order to check effects of overestimation of the exchange splitting in the QSGW[13, 23, 25], we use the linear mixing of the 20% LDA exchange correlation as we already explained when we discuss ϵ_2, and calculate the spin-wave dispersion. Then it reduces the spin-wave dispersion by ∼ 11 %, thus our conclusion here is unchanged. Our results for the spin-wave dispersion in the QSGW can be understood as a result of the reduction of the anti-ferromagnetic contribution of the t_{2g} bands because of their large exchange splitting.

As a summary, our result for the spin-wave dispersions in the QSGW is clearly in contradiction to the experiments [36, 37, 38]. In contrast, we have shown that the quasiparticle levels and ϵ_2 are reasonable and consistent with experiments. Therefore we conjecture that it is necessary to include the degree of freedom of phonons through the magnon-phonon interaction so as to resolve the contradiction. In fact, [39, 40] had already suggested that the magnon-phonon interaction can change the spin-wave dispersions largely by the strong hybridization with phonons of the Jahn-Teller distortion. In contrast, the magnon-phonon interaction was supposed to play a much smaller role for the spin-wave dispersion in some experimental works than our result suggests: For example, Dai et al [37] and Ye et al [36] claimed only the softening around the BZ boundaries are attributed to the hybridization: Moussa claimed that the spin-wave disper-

sion is little affected by the magnon-phonon interaction [38].

In conclusion, the QSGW gives a very different picture from the LDA for the physics of $La_{1-x}A_xMnO_3$. The main difference from LDA is as for the magnitude of the exchange splitting for the t_{2g} band. It is $\sim$2 eV larger than that in the LDA. QSGW predicts a large gap in the minority spin (i.e., it is fully polarized). Our results are consistent with the ARPES and the optical measurements, but not with the spin-wave measurements. We think that this disagreement indicates a very strong hybridization of spin wave with the Jahn-Teller type of phonons. It should be necessary to evaluate its effect based on a reliable first-principle method.

We thank to Prof. M. van Schilfgaarde for helping us to use his code for full-potential Linear muffin-tin orbital method. This work was supported by DOE contract DE-FG02-06ER46302, and by a Grant-in-Aid for Scientific Research in Priority Areas "Development of New Quantum Simulators and Quantum Design" (No.17064017) of The Ministry of Education, Culture, Sports, Science, and Technology, Japan. We are also indebted to the Ira A. Fulton High Performance Computing Initiative.

[1] Y. Tokura and N. Nagaosa, Science **288** (2000).
[2] M. Imada, A. Fujimori, and Y. Tokura, Rev. Mod. Phys. **70**, 1039 (1998).
[3] S.-W. Cheong and M. Mostovoy, Narure materials **6**, 13 (2007).
[4] R. Ramesh and N. A. Spaldin, Narure materials **6**, 21 (2007).
[5] H. Sawada, Y. Morikawa, K. Terakura, and N. Hamada, Phys. Rev. B **56**, 12154 (1997).
[6] I. Solovyev, N. Hamada, and K. Terakura, Phys. Rev. B **53**, 7158 (1996).
[7] I. V. Solovyev and K. Terakura, Phys. Rev. Lett. **82**, 2959 (1999).
[8] Z. Fang, I. V. Solovyev, and K. Terakura, Phys. Rev. Lett. **84**, 3169 (2000).
[9] P. Ravindran, A. Kjekshus, H. Fjellvåg, A. Delin, and O. Eriksson, Phys. Rev. B **65**, 064445 (2002).
[10] K. Terakura, T. Oguchi, A. R. Williams, and J. Kübler, Phys. Rev. B **30**, 4734 (1984).
[11] K. Terakura, A. R. Williams, T. Oguchi, and J. Kübler, Phys. Rev. Lett. **52**, 1830 (1984).
[12] S. V. Faleev, M. van Schilfgaarde, and T. Kotani, Phys. Rev. Lett. **93**, 126406 (2004).
[13] T. Kotani, M. van Schilfgaarde, and S. V. Faleev, Physical Review B **76**, 165106 (pages 24) (2007).
[14] I. V. Solovyev and K. Terakura, Phys. Rev. B **58**, 15496 (1998).
[15] T. Kotani and M. van Schilfgaarde, Journal of Physics: Condensed Matter **20**, 295214 (2008), URL `http://stacks.iop.org/0953-8984/20/295214`.
[16] V. I. Anisimov, F. Aryasetiawan, and A. I. Lichtenstein, J. Phys.: Condens. Matter **9**, 767 (1997).
[17] H. Sawada and K. Terakura, Phys. Rev. B **58**, 6831 (1998).
[18] M. Korotin, T. Fujiwara, and V. Anisimov, Phys. Rev. B. **62**, 5696 (2000).
[19] T. Kotani, J.Phys. Cond. Mat. **12** (2000).
[20] T. Miyake and F. Aryasetiawan, Physical Review B (Condensed Matter and Materials Physics) **77**, 085122 (pages 9) (2008), URL `http://link.aps.org/abstract/PRB/v77/e085122`.
[21] T. Kotani and M. van Schilfgaarde, Solid State Commun. **121**, 461 (2002).
[22] A. N. Chantis, M. van Schilfgaarde, and T. Kotani, Physical Review B **76**, 165126 (2007).
[23] M. Shishkin, M. Marsman, and G. Kresse, Physical Review Letters **99**, 246403 (pages 4) (2007).
[24] F. Bruneval, N. Vast, and L. Reining, Physical Review B **74**, 045102 (pages 15) (2006).
[25] M. van Schilfgaarde, T. Kotani, and S. Faleev, Phys. Rev. Lett. **96**, 226402 (pages 4) (2006).
[26] M. van Schilfgaarde, T. Kotani, and S. V. Faleev, phys. Rev. B. (2006), in press. Preprint cond-mat/0508295.
[27] T. Kotani, M. van Schilfgaarde, S. V. Faleev, and A. Chantis, Journal of Physics: Condensed Matter **19**, 365236 (8pp) (2007).
[28] A. N. Chantis, M. van Schilfgaarde, and T. Kotani, Phys. Rev. Lett. **96**, 086405 (2006).
[29] B. Dabrowski, K. Rogacki, X. Xiong, P. W. Klamut, R. Dybzinski, J. Shaffer, and J. D. Jorgensen, Phys. Rev. B **58**, 2716 (1998).
[30] H. Kino, F. Aryasetiawan, I. Solovyev, T. Miyake, T. Ohno, and K. Terakura, Physica B - condensed matter **329**, 858 (2003).
[31] Y. Nohara, A. Yamasaki, S. Kobayashi, and T. Fujiwara, Physical Review B (Condensed Matter and Materials Physics) **74**, 064417 (pages 6) (2006), URL `http://link.aps.org/abstract/PRB/v74/e064417`.
[32] M. I. Katsnelson, V. Y. Irkhin, L. Chioncel, A. I. Lichtenstein, and R. A. de Groot, Reviews of Modern Physics **80**, 315 (pages 64) (2008), URL `http://link.aps.org/abstract/RMP/v80/p315`.
[33] R. Liu, W. C. Tonjes, C. G. Olson, J. J. Joyce, A. J. Arko, J. J. Neumeier, J. F. Mitchell, and H. Zheng, Journal of Applied Physics **88**, 786 (2000).
[34] A. Chikamatsu, H. Wadati, H. Kumigashira, M. Oshima, A. Fujimori, N. Hamada, T. Ohnishi, M. Lippmaa, K. Ono, M. Kawasaki, et al., Physical Review B **73**, 195105 (pages 7) (2006).
[35] Y. Okimoto, T. Katsufuji, T. Ishikawa, T. Arima, and Y. Tokura, Phys. Rev. B **55**, 4206 (1997).
[36] F. Ye, P. Dai, J. A. Fernandez-Baca, D. T. Adroja, T. G. Perring, Y. Tomioka, and Y. Tokura, Physical Review B **75**, 144408 (pages 10) (2007).
[37] P. Dai, H. Y. Hwang, J. Zhang, J. A. Fernandez-Baca, S.-W. Cheong, C. Kloc, Y. Tomioka, and Y. Tokura, Phys. Rev. B **61**, 9553 (2000).
[38] F. M. et al.and M. Hennion, P. Kober-Lehouelleur, D. Reznik, S. Petit, H. Moudden, A. Ivanov, Y. M. Mukovskii, R. Privezentsev, and F. Albenque-Rullier, Physical Review B **76**, 064403 (pages 9) (2007).
[39] L. M. Woods, Phys. Rev. B **65**, 014409 (2001).

[40] T.-M. Cheng and L. Li, Journal of Magnetism and Magnetic Materials **320**, 1 (2008).